Structure−Function Studies of Human Apolipoprotein A-V: A Regulator of Plasma Lipid Homeostasis†

Jennifer A. Beckstead,‡ Michael N. Oda,‡ Dale D. O. Martin,‡ Trudy M. Forte,§ John K. Bielicki,§ Trish Berger,|| Robert Luty,⊥ Cyril M. Kay,⊥ and Robert O. Ryan*,‡

Lipid Biology in Health and Disease Research Group, Children's Hospital Oakland Research Institute, Oakland, California 94609, Genome Sciences Department, Life Science Division, Lawrence Berkeley National Laboratory, Berkeley, California 94720, Department of Animal Science, University of California, Davis, California 95616, and Department of Biochemistry and Protein Engineering Network of Centers of Excellence, University of Alberta, Edmonton, Alberta T6G 2S2, Canada

Received March 31, 2003; Revised Manuscript Received June 9, 2003

ABSTRACT: To investigate structure and function relations of a new member of the exchangeable apolipoprotein family that modulates plasma lipid levels, recombinant human apolipoprotein (apo) A-V was produced in *Escherichia coli* and isolated by a combination of nickel chelation affinity chromatography and reversed-phase HPLC. Antibodies directed against apoA-V were generated and employed in immunoblotting experiments. Anti-apoA-V IgG gave a strong response against recombinant apoA-V from *E. coli* and human apoA-V expressed in transgenic mice, but did not recognize human apoA-I or apoA-IV. In neutral-pH buffers, at concentrations of >0.1 mg/mL, isolated lipid-free apoA-V is poorly soluble. By contrast, apoA-V is soluble in 50 mM sodium citrate (pH 3.0). Far-UV circular dichroism analysis and spectral deconvolution reveal that apoA-V possesses 32% α-helix, 33% β-sheet, 16% β-turn, and 18% random coil secondary structure conformers. Temperature-induced denaturation studies gave rise to a transition midpoint of 47.1 °C. Upon being cooled to ambient temperature from 85 °C, apoA-V failed to recover all of the negative ellipticity present in unheated apoA-V. ApoA-V interacts with bilayer vesicles of dimyristoylphosphatidylcholine to form discoidal complexes with diameters in the range of 15−20 nm. However, apoA-V was a poor activator of lecithin:cholesterol acyltransferase where the activity was 8.5 ± 1.8% of that of apoA-I. Furthermore, apoA-V failed to support enhanced efflux of cholesterol from cAMP-treated J774 macrophages, although low levels of efflux were obtained from unstimulated cells. Taken together, the results demonstrate recombinant apoA-V possesses unique structural and functional characteristics, in keeping with its proposed role in the modulation of plasma lipid levels.

The exchangeable apoliproproteins play a critical role in plasma lipoprotein metabolism. As many as 11 different exchangeable apolipoproteins have been identified and characterized from human plasma, and these generally possess a common structural motif, the amphipathic α-helix (*1*). Given their fundamental and essential role in plasma lipoprotein metabolism, it is generally recognized that aberrations in exchangeable apolipoprotein concentration or structure can lead to dyslipidemia and premature atherosclerosis. For example, using gene disruption techniques, it has been shown that a deficiency in apoE leads to severe hypercholesterolemia and premature atherosclerosis (*2, 3*). On the other hand, apoA-I and apoA-IV transgenic mice were protected from diet-induced atherosclerosis (*4, 5*).

Recently, a new member of the exchangeable apolipoprotein family was discovered. In a comparative genomics study designed to identify evolutionarily conserved sequences with potential function, Pennacchio et al. (*6*) determined the sequence of 200 kb of mouse DNA in a region orthologous to the human apolipoprotein gene cluster (apoA-I/C-III/A-IV) on human chromosome 11q23. By comparison of mouse and human sequence data, a region of interspecies sequence conservation was discovered approximately 30 kb proximal to the apolipoprotein gene cluster. Further analysis revealed that this genomic interval contained a putative apolipoprotein-like gene (termed apoA-V). Further characterization of this region of the mouse sequence, as well as expressed sequence tag information, indicated the presence of four exons containing a 1107 bp open reading frame. The sequence of the predicted 368-amino acid protein was homologous to those of known apolipoproteins. The highest level of homology (24% identical and 49% similar) was observed with mouse apolipoprotein A-IV. Analysis of the orthologous human genomic structure revealed a similar gene structure and predicted the presence of an open reading frame

† This work was supported by grants from the American Heart Association (0255958Y) and the National Institutes of Health (HL64159 and HL 55493) and the Protein Engineering Network of Centers of Excellence.

* To whom correspondence should be addressed: Children's Hospital Oakland Research Institute, 5700 Martin Luther King Jr. Way, Oakland, CA 94609. Telephone: (510) 450-7645. Fax: (510) 450-7910. E-mail: rryan@chori.org.

‡ Children's Hospital Oakland Research Institute.

§ Lawrence Berkeley National Laboratory.

|| University of California.

⊥ University of Alberta.

10.1021/bi034509t CCC: $25.00
Published on Web 07/15/2003

encoding a 366-amino acid protein that is 71% homologous to mouse apoA-V.

To evaluate the physiological role of apoA-V, Pennacchio et al. (*6*) generated transgenic mice that overexpress the human apoA-V protein as well as mice lacking apoA-V using gene disruption techniques. Profound effects were observed in both transgenic and knockout mice. ApoA-V transgenic mice displayed a plasma triacylglycerol (TG)[1] level 3-fold lower than that of control littermates. By contrast, apoA-V knockout mice revealed a plasma TG level 4-fold higher than that of controls. Levels of very low-density lipoprotein (VLDL) particles were increased in the homozygous knockout mice and decreased in the transgenic mice, compared to controls. In the heterozygous knockout mouse, VLDL levels were intermediate between those of the homozygous knockout and control mouse. Using cDNA subtraction techniques, van der Vliet et al. (*7*) demonstrated that mRNA encoding a novel gene, identified as apoA-V, was upregulated following partial hepatectomy. The apoA-V protein was secreted by the liver and was transported primarily on large high-density lipoprotein (HDL). In subsequent adenoviral-mediated transfection experiments, van der Vliet et al. (*8*) induced a 20-fold increase in apoA-V plasma concentrations that resulted in a 70% decrease in TG levels.

The association of apoA-V with HDL in the mouse and rat suggests that the protein possesses lipid binding properties similar to those of other exchangeable apolipoproteins. Its HDL association may also be important in the interaction of the protein with membrane lipids where it may have a role in cholesterol efflux or facilitated lipid exchange reactions. This HDL association might also be linked with an ability of apoA-V to activate lecithin:cholesterol acyltransferase (LCAT) since both apoA-I and apoA-IV have this capability. To investigate apoA-V structure and function relations, we constructed a plasmid vector for expression of recombinant human apoA-V in bacteria. As reported here, recombinant apoA-V possesses hallmark features of an exchangeable apolipoprotein yet possesses unique characteristics that may ultimately be important to the mechanism whereby it modulates plasma lipid homeostasis.

EXPERIMENTAL PROCEDURES

ApoA-V/pET Plasmid Vector. The coding sequence of human apoA-V (a kind gift of E. Rubin and L. Pennacchio) was amplified using synthetic oligonucleotide primers and inserted into the pBluescript KS(+) vector (Stratagene, La Jolla, CA). Manipulations of the DNA sequence were performed in this plasmid, which was propagated in *Escherichia coli* DH5α cells. DNA sequencing was performed to verify that no unwanted mutations occurred during the process of plasmid vector construction. For protein expression, the apoA-V cDNA was subcloned into the pET 20b+ plasmid (Novagen, Madison, WI) to yield the pET/A-V vector. Mouse plasma samples were obtained from L. Pennacchio (Lawrence Berkeley National Laboratory).

Expression and Purification of Recombinant apoA-V. ApoA-V expression and purification were performed according to the methods of Ryan et al. (*9*) with some modification. Briefly, *E. coli* BL21(DE3)pLysS cells bearing the pET/A-V plasmid were cultured in 500 mL of NCZYM medium (with 50 μg/mL ampicillin) at 37 °C. When the culture OD_{600} reached 0.6, apoA-V synthesis was induced by the addition of isopropyl thiogalactopyranoside to a final concentration of 0.5 mM. After 3 h, the bacteria were pelleted by centrifugation and disrupted by sonication. The cell lysate was centrifuged at 20000*g* for 30 min at 4 °C. The supernatant fraction was then mixed with an equal volume of phosphate-buffered saline containing 6 M guanidine HCl and applied to a 5 mL bed volume Hi-Trap affinity column (Amersham Pharmacia Biotech), washed with 2 column volumes of buffer (containing 3 M guanidine HCl and 40 mM imidazole), and eluted in a buffer containing 3 M guanidine HCl and 500 mM imidazole. Fractions containing the apoA-V protein were pooled and dialyzed against deionized water, resulting in precipitation of the protein. The sample was redissolved in 0.05% trifluoroacetic acid in water (or 0.1 N HCl) and further purified on a Perkin-Elmer Series 200 high-pressure liquid chromatograph. The sample was applied to an RXC-8 Zorbax 300SB semipreparative column and eluted with a linear AB gradient of 2% B/min, where solvent A was 0.05% trifluoroacetic acid in water and solvent B was 0.05% trifluoroacetic acid in acetonitrile. Fractions were monitored at 230 nm, and those containing apoA-V were pooled, lyophilized, and stored at −20 °C.

Antibody Generation. Purified recombinant human apoA-V (200 μg of protein) was emulsified in adjuvant and injected into a goat. Four weeks later, an additional injection (200 μg of protein) emulsified in adjuvant was given. Seven weeks after the initial injection, 200 mL of serum was collected. An aliquot of goat anti-apoA-V serum was passed over a 5 mL Hi-Trap Protein G HP column (Amersham Pharmacia Biotech). The IgG fraction present in the serum sample was bound to the column in buffer [20 mM sodium phosphate (pH 7.0)] and, after washing, eluted with 0.1 M glycine (pH 2.5) directly into tubes containing 200 μL of 1 M Tris-HCl (pH 9.0). IgG recovered from the column was equilibrated in 20 mM sodium phosphate (pH 7.0). Subsequently, the IgG fraction was biotinylated by incubation for 15 min with 5 mL of 0.5 mg/mL sulfo-NHS-SS-biotin (Pierce Chemical Co.) in borate buffer on a rocking platform with slow agitation. Unreacted biotin reagent was quenched with buffer supplemented with 100 mM glycine. After removal of the quenching medium, labeled IgG was dialyzed into 20 mM sodium phosphate (pH 7.0), aliquoted, and stored at −80 °C.

Immunoblotting. For immunoblotting, protein samples were run on a 4 to 20% acrylamide gradient, Tris-glycine SDS slab gel (Invitrogen Life Tech). Separated proteins were transferred to a 0.2 μm PVDF membrane (Bio-Rad Laboratories) using the blot module Electro-Eluter (Bio-Rad Laboratories) at a constant current of 150 mA for 3 h. Nonspecific binding sites on the membrane were blocked with 0.1% TTBS [0.1% Tween 20, 20 mM Tris, and 150 mM NaCl (pH 7.2)] overnight, at room temperature while the mixture was being rotated. Biotinylated apoA-V IgG (1:10000 dilution in 0.1% TTBS) was incubated with the membrane for 60 min while the mixture was being rotated.

[1] Abbreviations: apo, apolipoprotein; SDS, sodium dodecyl sulfate; PAGE, polyacrylamide gel electrophoresis; CD, circular dichroism; TG, triacylglycerol; HDL, high-density lipoprotein; VLDL, very low-density lipoprotein; TTBS, Tween with Tris-buffered saline; DMPC, dimyristoylphosphatidylcholine; SDS, sodium dodecyl sulfate; PAGE, polyacrylamide gel electrophoresis.

After the mixture had been washed three times in TTBS, avidin-D with the horseradish peroxidase conjugate (Vector Laboratories; diluted 1:30 in 0.1% TTBS) was incubated with the membrane for 60 min. Subsequently, the membrane was washed three times in TTBS and incubated with SuperSignal West Femto Maximum Sensitivity Substrate (Pierce Chemical Co.) in which both reagents were diluted by adding 0.5 mL in 9 mL of dH_2O. The substrate was incubated for 2−5 min at room temperature and exposed to CL-Xposure Film (Pierce Chemical Co.) for 60 s. Film was developed using a Kodak M35A X-OMAT processor.

Analytical Procedures. Protein concentrations were determined using the bicinchoninic acid assay (Pierce Chemical Co.) using bovine serum albumin as a standard. SDS−PAGE was performed on 4 to 20% acrylamide slab gels run at a constant current of 30 mA for 1.5 h. Gels were stained with Coomassie Brilliant Blue R-250, and the relative mobility of protein samples was compared to that of known standards (Bio-Rad low-molecular weight standards). ApoA-V solubility studies were conducted at various pH values employing 50 mM sodium citrate, sodium phosphate, or Tris (with 150 mM NaCl) within the pH range of 2.5−9.5.

Circular Dichroism Spectroscopy. Far-UV circular dichroism (CD) measurements were performed on a Jasco J-720 spectropolarimeter using Jasco J-700 Hardware Manager Software (version 1.10.00) on a Pentium computer (Windows98). The spectropolarimeter was routinely calibrated using a 0.06% (w/v) aqueous solution of ammonium *d*-10-camphor sulfonate at 290.5 nm. Scans were performed using a 0.02 cm path length cuvette and a protein concentration of 21.5 μM. The sample chamber was maintained at 25 °C using a Lauda RM6 refrigerated recirculating water bath. Temperature denaturation scans were performed using a 0.10 cm path length cuvette in a Jasco Peltier-type thermostatic cell holder and a protein concentration of 6.64 μM. All protein samples were dissolved in 50 mM sodium citrate (pH 3.0). The concentrations of apoA-V stock solutions were determined hydrodynamically by fringe count in a Beckman XLI analytical ultracentrifuge according to the method of Babul and Stellwagen (*10*). Baseline correction, noise reduction, and ellipticity calculations for the scans were carried out using Jasco J-700 for Windows Standard Analysis Software (version 1.20.00). The values are shown as mean residue molar ellipticity (millidegrees centimeter squared per decimole) calculated as

$$[\theta] = (\mathrm{MRW})(\theta_{222})/(10lc)$$

where $[\theta]$ is the mean residue ellipticity, MRW is the mean residue weight (taken to be 113.403), θ_{222} is the measured ellipticity at 222 nm in millidegrees, l is the cuvette path length in centimeters, and c is the protein concentration in milligrams per milliliter. Deconvolution was performed on the scans using the Contin program of Provencher and Glöckner (*11*).

Analytical Ultracentrifugation. Sedimentation equilibrium experiments were conducted at 30 °C in a Beckman XL-I analytical ultracentrifuge using interference optics, as described by Laue and Stafford (*12*). Aliquots (110 μL) of the sample solution were loaded into six-sector CFE sample cells, allowing three concentrations of sample to be run simultaneously. Runs were performed at a minimum of two different speeds, and each speed was maintained until there was no significant difference in $r^2/2$ versus absorbance scans taken 2 h apart to ensure that equilibrium was achieved. The sedimentation equilibrium data were evaluated using the NONLIN program, which incorporates a nonlinear least-squares curve fitting algorithm described by Johnson et al. (*13*). This program allows the analysis of both single and multiple data files. Data can be fit to either a single-ideal species model or models containing up to four associating species, depending on which parameters are permitted to vary during the fitting routine. The protein's partial specific volume and the solvent density were estimated using the SEDNTERP program, which incorporates calculations described in detail by Laue et al. (*14*).

Interaction of ApoA-V with the Phospholipid. Bilayer vesicles of dimyristoylphosphatidylcholine (DMPC) were prepared by extrusion as described elsewhere (*15*) in 50 mM sodium citrate and 150 mM NaCl (pH 3.0). Vesicles were incubated with apoA-V (2.5:1, w/w) at 24 °C for 16 h. Following incubation, the sample was adjusted to 1.31 g/mL by the addition of solid KBr (final volume of 2.5 mL), transferred to a 5.1 mL centrifuge tube, overlayered with 2.5 mL of saline, and centrifuged at 275000*g* for 5 h in a Beckman VTi 65.2 rotor. The tube contents were fractionated (0.5 mL), and those containing phospholipid and protein were combined, dialyzed into phosphate-buffered saline, and stored at 4 °C. The size distribution of DMPC−apoA-V complexes was evaluated by nondenaturing gradient PAGE as described by Nichols et al. (*16*). The morphology of complexes was determined by negative stain electron microscopy as previously described (*17*).

Lecithin:Cholesterol Acyltransferase Activity Assays. The ability of apoA-V to activate lecithin:cholesterol acyltransferase (LCAT) was examined using recombinant LCAT obtained from CHO-K1 cells stably transfected with human LCAT cDNA (a kind gift of J. Parks). Cholesterol esterification was assessed using the exogenous substrate procedure described by Chen and Albers (*18*). Proteoliposomes composed of either apoA-V or apoA-I were prepared using egg yolk phosphatidylcholine (PC) and unesterified cholesterol (1:250:12.5 molar ratios) containing trace amounts of [^{14}C]-cholesterol as previously described (*19*). Proteoliposomes were exposed to increasing concentrations (0.2−1.0 μg) of purified LCAT protein to measure initial reaction rates in incubation mixtures containing human serum albumin (0.5%), β-mercaptoethanol (5 mM), and Tris (20 mM)-buffered saline EDTA (2.7 mM) (pH 8.0). Incubations were performed at 37 °C for 0.5 h. Lipids were extracted with hexane and separated by TLC using toluene as the mobile carrier solvent. Results were expressed as a percentage of the amount of the initial [^{14}C]cholesterol converted to [^{14}C]cholesteryl ester.

Cellular Cholesterol Efflux. J774 macrophages were used to assess the capacity of apoA-V to promote cholesterol efflux. Cells were plated at an initial density of 1×10^6 cells mL^{-1} well^{-1} in 24-well culture plates and allowed to grow (48 h) to confluent monolayers in RPMI medium containing 1% fetal bovine serum and 1 μCi mL^{-1} well^{-1} of [^{3}H]-cholesterol as described previously (*20*). The cAMP analogue 8-(4-chlorophenylthio)adenosine 3′,5′-cyclic monophosphate (0.3 mM) was used to upregulate the ABCA1 transporter (*21*). Recombinant human apoA-I was used as a control. Lipid-free apoA-V (25 μg/mL) and apoA-I (25 μg/mL) were

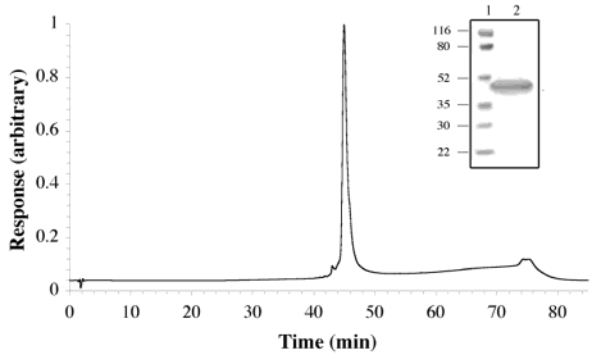

FIGURE 1: Reversed-phase HPLC of recombinant human apoA-V. The protein was loaded onto a Vydac C8 column and eluted with a gradient of water and acetonitrile (0.05% trifluoroacetic acid) from 0 to 100% acetonitrile. The inset shows SDS−PAGE analysis of recombinant apoA-V: (lane 1) molecular weight standards and (lane 2) 10 μg of apoA-V.

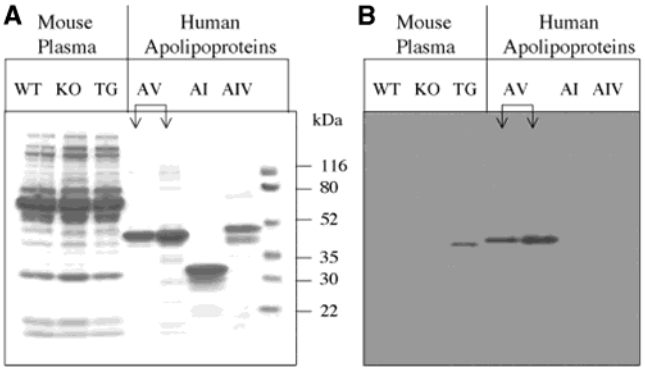

FIGURE 2: Immunoblot analysis of apoA-V. Proteins were separated on 4 to 20% acrylamide gradient gels and (A) stained with Commassie Blue or (B) transferred to a PVDF membrane and probed with biotinylated anti-apoA-V IgG. Sample loads on the immunoblot: 0.5 μL of mouse plasma, 1 and 2 ng of apoA-V (see arrows), 100 ng of apoA-I, and 100 ng of apoA-IV.

added to serum-free RPMI and filter sterilized (0.45 μm) before additions to cells. Filtration did not remove any apoA-V (judged by Western blot analysis), indicating apoA-V solubility in serum-free medium at this concentration. Aliquots of efflux medium were removed at various times, and cellular debris was removed by centrifugation (1000*g* for 8 min at 4 °C). Radioactivity in medium supernatant was quantified, and efflux results were expressed as a percentage of the cellular [^{3}H]cholesterol released into the medium as a function of time.

RESULTS

Expression and Isolation of ApoA-V. The cDNA encoding human apoA-V was introduced into the pET 20b expression vector immediately downstream from an in-frame His tag-encoding sequence. When the fusion protein was expressed under standard conditions developed for recombinant human apolipoprotein A-I (*9*), we noted that the yield of the recombinant protein was quite low. Whereas significant amounts of apoA-V were present in the crude bacterial pellet, the intact protein was not recovered in the eluate from the nickel chelation affinity chromatography column. Investigation of this phenomenon revealed that recombinant apoA-V bound to the nickel chelation column is subject to degradation when the column contents are exposed to buffer lacking guanidine HCl. Because the original protocol that was employed included removal of guanidine HCl prior to protein elution with imidazole, poor yields of apoA-V were observed. Two major breakdown products were characteristically observed using this protocol, an 11 kDa band and a 30 kDa band. On the other hand, when 6 M guanidine HCl was included in all buffers used during this chromatography step, the yield of intact apoA-V was substantially improved. Further purification by reversed-phase HPLC resulted in an apoA-V preparation that gave rise to a single major band when analyzed by SDS−PAGE (Figure 1). Using this protocol, yields of recombinant apoA-V were 3−5 mg/L of bacterial culture.

An antibody to recombinant human apoA-V was generated, and Figure 2 depicts a gel stained with Coomassie Blue and a corresponding immunoblot. No reactivity was observed in either control mouse plasma or apoA-V knockout mouse plasma. On the other hand, in the case of human apoA-V transgenic mouse plasma, the antibody recognized a single band corresponding to the molecular weight of apoA-V. In addition, the immunoblot contained different amounts of isolated recombinant apoA-V as well as two other members of the human apolipoprotein family, apoA-I and apoA-IV. Whereas anti-apoA-V IgG recognized as little as 1 ng of apoA-V, no reactivity was observed toward apoA-I or apoA-IV at 100 ng sample loads. These results indicate that the antibody is specific for apoA-V.

ApoA-V Properties. Whereas apoA-V was soluble in 50 mM sodium citrate (pH 3.0), it was insoluble in neutral-pH buffers at concentrations of >0.1 mg/mL. To characterize the solubility properties of apoA-V, the effect of solution pH on the solubility of apoA-V was determined. It was observed that between the pH limits of 3.5 and 9.0 apoA-V is largely insoluble. The poor solubility of apoA-V around neutral pH values may be attributed to its pI of 6.2. On the other hand, the presence of a 17-residue N-terminal His tag extension on the protein could conceivably affect its solubility properties. An engineered thrombin cleavage site at the junction between the His tag and apoA-V could not be used in the case of lipid-free apoA-V because of the insolubility of apoA-V at pH 8 together with the lack of thrombin activity at pH 3. However, when associated with DMPC, apoA-V is soluble at neutral pH, and thrombin digestion of DMPC-bound apoA-V resulted in efficient removal of the His tag. Following delipidation and re-isolation by reversed-phase HPLC, the solubility properties of apoA-V were unchanged. Thus, we conclude that the His tag extension is not responsible for the lack of solubility of lipid-free apoA-V at neutral pH values. Sequence analysis indicates that apoA-V does not possess predicted transmembrane segments and lacks consensus sites for N-linked glycosylation or lipid modification. Thirty percent of the amino acids in mature human apoA-V possess charged side chains at neutral pH (49 Glu/Asp and 41 Arg/Lys) that, together with the 14 His residues that are present, are relative proportions that are similar to those found in other apolipoproteins. It is conceivable that apoA-V maintains solubility in plasma through interaction with lipoproteins.

CD Spectrum of ApoA-V. A far-UV CD spectrum of apoA-V is depicted in Figure 3. The spectrum reveals molar ellipticity minima at 208 and 222 nm, indicative of the presence of α-helix secondary structure. Deconvolution of the spectrum with the Contin program of Provencher and

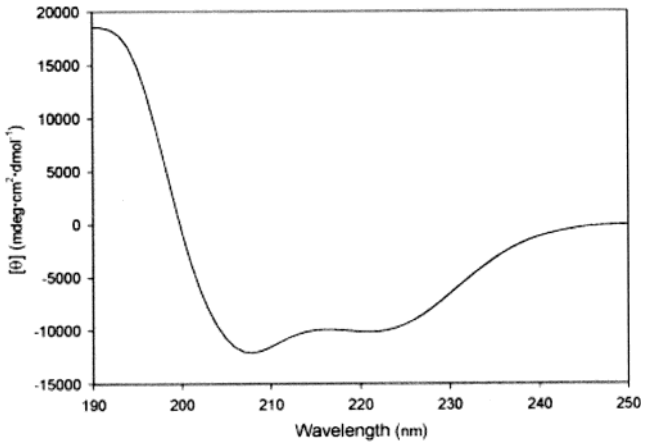

FIGURE 3: Far-UV CD spectroscopy of apoA-V. Spectra were collected at a protein concentration of 0.271 mg/mL at 25 °C.

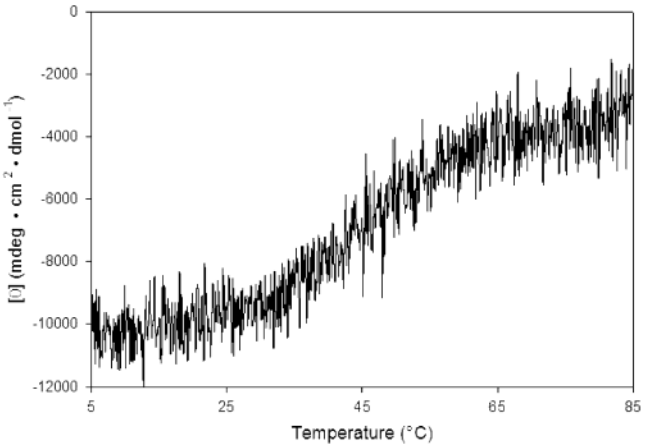

FIGURE 4: Temperature-induced denaturation of apoA-V. Data are presented as the mean residue molar ellipticity collected at 222 nm every 0.1 °C from 5 to 85 °C.

Glöckner (*11*) indicated that, at pH 3, apoA-V is comprised of 32% α-helix, 33% *β*-sheet, 16% *β*-turn, and 18% random coil. Thus, unlike most members of the exchangeable apolipoprotein family, apoA-V displays significant amounts of *β*-structure.

ApoA-V Stability Properties. To assess its stability properties in solution, the effect of temperature on the ellipticity of apoA-V was determined (Figure 4). As the temperature was increased from 5 to 37 °C, a small decrease in negative ellipticity was noted. However, above 37 °C, there was a much sharper temperature-dependent decrease in molar ellipticity, with a nearly complete loss of structure occurring at 60 °C. Between 60 and 85 °C, further losses in molar ellipticity were small. The general features of the temperature melt profile are consistent with a single native → unfolded transition with a midpoint of 47.1 °C. To evaluate the reversibility of temperature-induced unfolding of apoA-V, CD spectral scans were obtained before, during, and after a temperature melt (Figure 5). The results revealed that, although apoA-V recovers from the melt, it is unable to regain 100% of the molar ellipticity present in unheated apoA-V.

ApoA-V Self-Association. To investigate apoA-V self-association properties, sedimentation equilibrium experiments were performed in 50 mM sodium citrate (pH 3.0) at speeds of 8000 and 12 000 rpm and loading concentrations of 1.50, 2.70, and 5.88 mg/mL. A significant dependence on rotor speed and loading concentration was observed in the calculated apparent average molecular weights, ranging from 330 000 at 8000 rpm to 68 000 at 12 000 rpm. It was not possible to obtain a good fit to any of the self-association models when fitting all of the data sets globally using the NonLin program. Under these conditions, we conclude that apoA-V undergoes nonspecific aggregation at the concentrations used in these experiments. Further runs were performed with the inclusion of different concentrations of NaCl added to the buffer with no effect on the association and aggregation phenomenon.

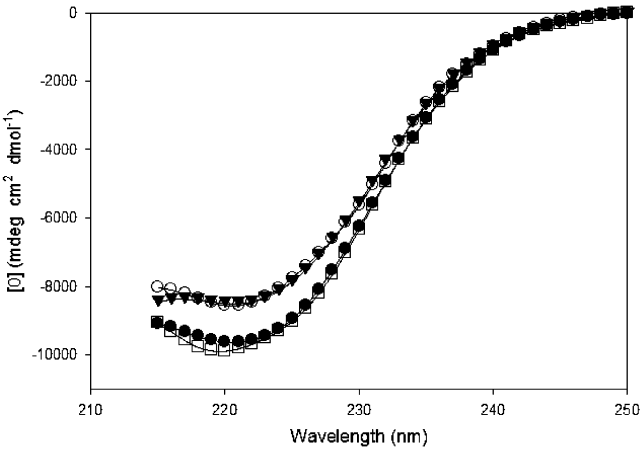

FIGURE 5: Recovery of ellipticity after a temperature melt. Far-UV CD scans (from 250 to 215 nm) of apoA-V were collected before, during, and after the temperature melt: initial scan at 25 °C (●), scan after cooling to 5 °C and returning to 25 °C (□), scan after heating to 85 °C and returning to 25 °C (○), and scan after equilibration for an additional 30 min at 25 °C (▼).

Binding of ApoA-V to Phospholipid. Upon incubation with bilayer vesicles of DMPC at a 1:1 weight ratio, apoA-V interacts with the phospholipid to form a discrete population of lipid particles (Figure 6). Native gradient PAGE analysis of the isolated lipid particles revealed a Stokes diameter in the range of 15−20 nm. Negative stain electron microscopy of the particles corroborated the size measurements and revealed disk-shaped particles that stack to form rouleaux. This result is similar to results obtained with other exchangeable apolipoproteins and is consistent with observations that apoA-V is found in association with HDL. Unlike lipid-free apoA-V, DMPC-bound apoA-V is soluble at neutral pH, and CD analysis of apoA-V−DMPC disks at pH 7 (data not shown) indicated the presence of 50% α-helix secondary structure, an 18% increase compared to the level in lipid-free apoA-V.

LCAT Activation and Cholesterol Efflux Properties of ApoA-V. To evaluate the ability of apoA-V to serve as an activator of LCAT, purified apoA-V was used to prepare a proteoliposome substrate that was exposed to physiological concentrations of purified LCAT. Compared with apoA-I, apoA-V was a poor activator of LCAT, where the activity was 8.5 ± 1.8% ($n = 3$) of that of apoA-I. In studies of apolipoprotein-mediated cholesterol efflux, apoA-I was used as a positive control. ApoA-I is known to stimulate the efflux of cholesterol from cells through interaction with the ABCA1 transporter. Upregulation of ABCA1 by cAMP maximizes cholesterol efflux. As shown in Figure 7, apoA-V-mediated cholesterol efflux was unaffected by treatment of the cells

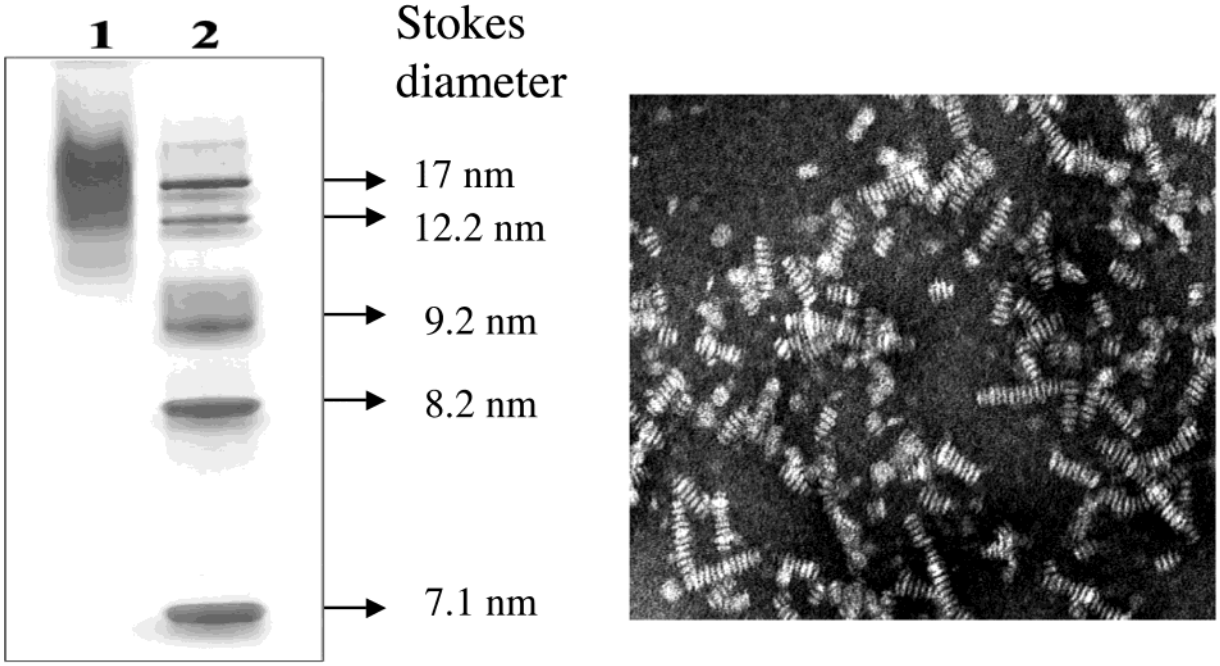

FIGURE 6: Characterization of apoA-V−DMPC complexes. (Left) Native gradient PAGE analysis of apoA-V−DMPC complexes prepared as described in Experimental Procedures: (lane 1) apoA-V−DMPC complexes and (lane 2) molecular size standards. (Right) Negative stain electron micrograph of apoA-V−DMPC complexes (magnification, 14.4 mm = 80 nm).

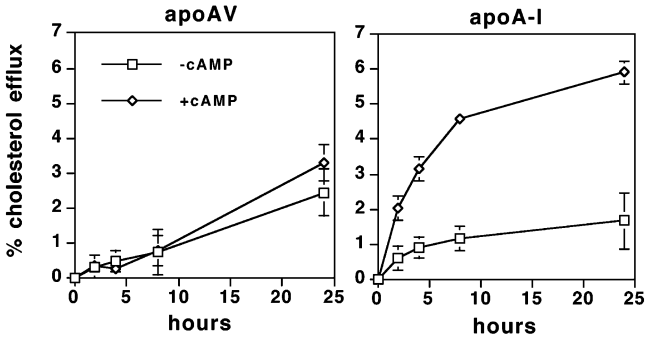

FIGURE 7: Efflux of cellular cholesterol to apolipoproteins. J774 mouse macrophages were prelabeled with [^{3}H]cholesterol and incubated with apoA-I (right) or apoA-V (left) in the absence (□) and presence (◇) of a cAMP analogue. Lipid-free recombinant apoA-I or apoA-V was added to cells at a final concentration of 25 μ/mL. Efflux observed in control incubations with serum-free medium was subtracted from that observed in incubations containing the apolipoprotein. Values that are reported are means ± the standard deviation of three separate experiments each performed in triplicate.

with cAMP and efflux levels were low. ApoA-I, on the other hand, shows the expected increase in the level of cellular cholesterol efflux in the presence of cAMP. The data suggest that cholesterol efflux to apoA-V occurs through an ABCA1-independent mechanism.

DISCUSSION

With the advent of the human genome project and the ability to compare large tracts of sequence across species, new opportunities for discovery of potentially important gene products exist. An excellent example of this concept emerged with the discovery of a previously unknown member of the exchangeable apolipoprotein family, apoA-V. Whereas genetic studies illustrate the important role played by apoA-V in plasma lipid metabolism, particularly TG metabolism (*6*, *22*, *23*), questions remain about the mechanism whereby apoA-V exerts its biological effects. The goal of determining how apoA-V influences plasma TG levels requires additional knowledge of the protein itself. In fact, previously, human apoA-V has not been isolated, and little is known of its structure, stability, lipid interaction properties, or potential regulatory effects.

Human apoA-V is synthesized with a cleavable signal peptide, comprising the first 23 amino acids of the protein sequence. This signal sequence directs the protein toward a secretory pathway, resulting in the appearance of apoA-V in plasma. To improve our understanding of apoA-V structure and function relationships, we created a vector construct for expression of human apoA-V in *E. coli*. Following optimization of the expression and purification protocol, yields of recombinant apoA-V in the range of 3−5 mg/L of bacterial culture were obtained. Recombinant apoA-V was used as an antigen to generate polyclonal antibodies in a goat. In characterization studies, it was shown that goat anti-human apoA-V IgG is specific for apoA-V and, thus, will likely be useful in future studies designed to quantitate apoA-V levels in human plasma samples and correlate these with TG levels. Whereas preliminary studies with human serum revealed specific reactivity against apoA-V, the present anti-human apoA-V IgG did not detect mouse apoA-V (Figure 2, wild-type mouse serum lane), suggesting either a lack of epitope conservation or that the amounts of apoA-V present are below the limits of detection.

In studies of apoA-V properties, results indicate the lipid-free protein is poorly soluble between the pH limits of 3.5 and 9 (at concentrations of >0.1 mg/mL). This solution behavior suggests human apoA-V may exist in association with lipoproteins in the plasma compartment, consistent with its observed plasma distribution in animal models (*6*, *7*). On the basis of the fact that apoA-V is a member of the apoA-I/C-III/A-IV gene family whose protein products belong to the exchangeable apolipoprotein family, studies were con-

ducted to characterize apoA-V in the lipid-free state. Far-UV CD spectroscopy of apoA-V in a buffer at pH 3 revealed the presence of different secondary structure elements, including α-helix, β-sheet, and β-turn. This result, together with the relatively large size of apoA-V, suggests apoA-V may possess more than one structural domain. Examination of its amino acid sequence reveals an unusual Ala_{292}-Pro-Pro-Pro-Pro-Gly_{297} segment in the C-terminal region of the protein. It is conceivable that the 47 residues beyond this tetraproline segment adopt an independent fold or may represent the 18% of apoA-V that exists as a random coil in the lipid-free state. Future studies of this peptide in isolation or a C-terminally truncated apoA-V may provide insight into the structural and/or biological role of this region of apoA-V. In the case of human apoA-I and apoE, their C-terminal regions are known to play a key role in lipoprotein binding and self-association in the absence of lipid (*24*, *25*). In a similar manner, apoA-V self-associates in the absence of lipid. As with other apolipoproteins, this may be a mechanism for sequestering lipid-binding sites on the protein from exposure to the aqueous milieu. Far-UV CD spectroscopy of DMPC-bound apoA-V indicates the acquisition of additional α-helix secondary structure, suggesting apoA-V undergoes a conformational change upon lipid association. At present, it is unknown which regions of apoA-V are responsible for self-association or lipid interaction. In the case of other exchangeable apolipoproteins, such as apoE, lipid interaction induces a conformational change in the protein whereby hydrophobic sites in the protein are exposed to the lipid surface (*26*). This bacterial expression system is ideally suited for experiments designed to determine which portions of apoA-V are responsible for self-association and lipid interaction, and these studies are in progress.

In the case of human apoA-I or insect apolipophorin III (*27*), it has been proposed that lipid interaction is facilitated by adoption of a loosely folded conformation in buffer. Secondary structure elements in both these proteins are stabilized by lipid association, and this may represent a driving force for their intrinsic lipid surface seeking property. Apolipophorin III exhibits a temperature-induced denaturation transition midpoint of 52 °C (*28*), while the corresponding value for apoA-I is 54 °C (*29*). Thermal denaturation experiments with apoA-V revealed a transition midpoint of 47.1 °C, consistent with a loosely folded structure in solution. Unlike human apoA-I or insect apolipophorin III, apoA-V was unable to fully recover 100% of its secondary structure elements following temperature-induced denaturation. Thus, apoA-V may possess a more complex tertiary fold, a portion of which is irreversibly altered, upon exposure to elevated temperatures. At present, it is not known if similar results will be observed with chaotrope-induced unfolding of apoA-V. In light of the fact that guanidine HCl exposure is employed in the protocol used for isolation of recombinant apoA-V, detailed characterization of the ability of apoA-V to recover a fully native conformation following such perturbations will be important in understanding the biological role of this protein.

The physicochemical properties of lipid-free apoA-V suggest that the protein has lipid binding activity. This was indeed demonstrated by apoA-V's ability to form lipid−protein complexes with DMPC. The complexes are similar to those formed with other exchangebable apolipoproteins and suggest that apoA-V binds to the lipid surface of lipoproteins, particularly HDL (*7*). Because apoA-V is transported on HDL and is structurally similar to other apolipoproteins such as apoA-IV and apoA-I that are known activators of LCAT, it is conceivable that it can serve to activate this enzyme. As reported herein, however, it is evident that this is not the case, suggesting that the structural motif required for LCAT activation is not present in this protein.

One of the characteristics of exchangeable apolipoproteins, including apoA-I and apoA-IV, is the ability to stimulate the efflux of cholesterol from cells via the ABCA1 transporter. However, the study presented here indicates that this is not the case for apoA-V. By contrast, apoA-V recruits low levels of cholesterol from cells, apparently by an ABCA1-independent mechanism. Thus, apoA-V appears to have detergent-like properties that allow it to remove membrane lipids in a nonspecific manner.

The fact that apoA-V is present at very low concentrations in plasma leaves open the question of its role in lipid metabolism, despite convincing studies in mice that show a correlation between apoA-V and TG levels. The availability of a recombinant apoA-V and a specific antibody will be useful for future studies in correlating apoA-V and TG levels in transgenic mice and humans and by allowing one to assess how apoA-V functions to modulate TG levels. In summary, we have developed a bacterial expression system for production of milligram quantities of human apoA-V. The recombinant protein was isolated and characterized in terms of its solution properties, secondary structure content, and thermal stability. In addition, we have generated an antibody directed against apoA-V that provides a potentially useful reagent for detection and quantification of apoA-V. Given the existing correlation between apoA-V and plasma TG in mouse models (*6*, *8*), human population studies designed to assess the significance of the correlation between apoA-V concentrations and plasma TG levels are possible. Because of the strong correlation between elevated plasma TG levels and cardiovascular disease, knowledge of how apoA-V modulates plasma TG levels may be of therapeutic significance.

ACKNOWLEDGMENT

We thank Drs. Len Pennacchio and Eddy Rubin for providing human apoA-V cDNA and aliquots of apoA-V transgenic and knockout mouse plasma. We also thank Dr. John Parks for providing LCAT, Dr. Richard Weinberg for apoA-IV, and Les Hicks for the sedimentation equilibrium analysis. We thank Barbara-Jean Nitta for assistance with antibody production. The expert animal care provided by the University of California at Davis goat facility is gratefully acknowledged. Finally, we thank Drs. Vasanthy Narayanaswami and Paul Weers for many helpful discussions.

REFERENCES

1. Segrest, J. P., Garber, D. W., Brouillette, C. G., Harvey, S. C., and Anantharamaiah, G. M. (1994) *Adv. Protein Res. 45*, 303−369.
2. Plump, A. S., Smith, J. D., Hayek, T., Aalto-Setala, K., Walsh, A., Verstuyft, J. G., Rubin, E. M., and Breslow, J. L. (1992) *Cell 71*, 343−353.
3. Zhang, S. H., Reddick, R. L., Piedrahita, J. A., and Maeda, N. (1992) *Science 258*, 468−471.

4. Rubin, E. M., Krauss, R. M., Sprangler, E. A., Verstuyft, J. G., and Clift, S. M. (1991) *Nature 353*, 265−267.
5. Duverger, N., Tremp, G., Caillaud, J.-M., Emmanuel, F., Castro, G., Fruchart, J.-C., Steinmetz, A., and Denefle, P. (1996) *Science 273*, 966−968.
6. Pennacchio, L. A., Olivier, M., Hubacek, J. A., Cohen, J. C., Cox, D. R., Fruchart, J. C., Krauss, R. M., and Rubin, E. M. (2001) *Science 294*, 169−173.
7. Van der Vliet, H. N., Sammels, M. G., Leegwater, A. C. J., Levels, J. H. M., Reitsma, P. H., Boers, W., and Chamulau, R. A. F. M. (2001) *J. Biol. Chem. 276*, 44512−44520.
8. Van der Vliet, H. N., Schaap, F. G., Levels, J. H., Ottenhoff, R., Looije, N., Wesseling, J. G., Groen, A. K., and Chamuleau, R. A. (2002) *Biochem. Biophys. Res. Commun. 295*, 1156−1159.
9. Ryan, R. O., Forte, T. M., and Oda, M. N. (2003) *Protein Expression Purif. 27*, 98−103.
10. Babul, J., and Stellwagen, E. (1969) *Anal. Biochem. 28*, 216−221.
11. Provencher, S. W., and Glöckner, J. (1981) *Biochemistry 20*, 33−37.
12. Laue, T. M., and Stafford, W. F., III (1999) *Annu. Rev. Biophys. Biomol. Struct. 28*, 75−100.
13. Johnson, M. L., Correia, J. J., Yphantis, D. A., and Halvorson, H. R. (1981) *Biophys. J. 36*, 575−588.
14. Laue, T. M., Shah, B. D., Ridgeway, T. M., and Pelletier, S. L. (1991) in *Analytical Ultracentrifugation in Biochemistry and Polymer Science* (Harding, S. E., Rowe, A. J., and Horton, J. C., Eds.) pp 90−125, Royal Society of Chemistry, Cambridge, England.
15. Weers, P. M. M., Narayanaswami, V., Kay, C. M., and Ryan, R. O. (1999) *J. Biol. Chem. 274*, 21804−21810.
16. Nichols, A. V., Krauss, R. M., and Musliner, T. A. (1986) *Methods Enzymol. 128*, 417−431.
17. Forte, T. M., and Nordhausen, R. W. (1986) *Methods Enzymol. 128*, 442−457.
18. Chen, C. H., and Albers, J. J. (1982) *J. Lipid Res. 23*, 680−691.
19. Bielicki, J. K., and Forte, T. M. (1999) *J. Lipid Res. 40*, 948−954.
20. Bielicki, J. K., and Oda, M. N. (2002) *Biochemistry 41*, 2089−2096.
21. Oram, J. F. (2002) *Curr. Opin. Lipidol. 13*, 373−381.
22. Talmud, P. J., Hawe, E., Martin, S., Olivier, M., Miller, G. J., Rubin, E. M., Pennacchio, L. A., and Humphries, S. E. (2002) *Hum. Mol. Genet. 15*, 3039−3046.
23. Nabika, T., Nasreen, S., Kobayashi, S., and Masuda, J. (2002) *Atherosclerosis 165*, 201−204.
24. Ji, Y., and Jonas, A. (1995) *J. Biol. Chem. 270*, 11290−11297.
25. Westerlund, J. A., and Weisgraber, K. H. (1993) *J. Biol. Chem. 268*, 15745−15750.
26. Weisgraber, K. H. (1994) *Adv. Protein Chem. 45*, 249−302.
27. Narayanaswami, V., and Ryan, R. O. (2000) *Biochim. Biophys. Acta 1483*, 15−36.
28. Ryan, R. O., Oikawa, K., and Kay, C. M. (1993) *J. Biol. Chem. 268*, 1525−1530.
29. Tall, A. R., Shipley, G. G., and Small, D. M. (1976) *J. Biol. Chem. 251*, 3749−3755.

BI034509T